cells or precursor cells, DNA methylation alterations are stably preserved on DNA double strands by covalent bonds. Therefore, even subtle alterations at the precancerous stage can be detected using highly sensitive methodology. DNA methylation alterations may be optimal indicators for carcinogenetic risk estimation.[12,13]

We have already established criteria for estimation of the risk of HCC development using bacterial artificial chromosome (BAC) array-based methylated CpG island amplification (BAMCA),[14–19] which can provide an overview of the DNA methylation tendency of individual large regions among all chromosomes;[13,19] 25 BAC clones, whose DNA methylation status was able to discriminate noncancerous liver tissue obtained from patients with HCCs in the learning cohort from normal liver tissue obtained from patients without HCCs, were identified.[18] However, sensitivity and specificity of such discrimination were not 100% in the validation cohort. Moreover, the CpG sites that are of diagnostic importance are unclear on each of the BAC clones with an average insert size of 170 kbp.[20] As the technique of BAMCA requires a large amount of genomic DNA and is somewhat cumbersome, risk estimation using BAMCA may be difficult to apply in a clinical setting.

Here, to identify precisely the CpG sites having the largest diagnostic impact, we quantitatively evaluated the DNA methylation status of 203 CpG sites on these 25 BAC clones using pyrosequencing in tissue specimens. Among the CpG sites, we were able to improve the specificity of carcinogenetic risk estimation by combining those showing the largest diagnostic impact and to apply such risk estimation to a very small amount of genomic DNA with a view to clinical application.

Material and Methods

Patients and tissue samples

As a learning cohort, 10 samples of normal liver tissue (C1–C10) showing no remarkable histological findings were obtained from specimens surgically resected from 10 patients without HCCs who were negative for both HBV surface antigen (HBs-Ag) and anti-HCV antibody (anti-HCV). The patients comprised seven men and three women with a mean (± standard deviation) age of 58.4 ± 9.7 years. Nine patients underwent partial hepatectomy for liver metastases of primary colon cancer, and one patient did so for liver metastases of a gastrointestinal stromal tumor of the stomach at the National Cancer Center Hospital, Tokyo, Japan. A total of 12 samples of noncancerous liver tissue (N1–N12) were obtained from 12 patients who underwent partial hepatectomy for HCCs. These patients comprised nine men and three women with a mean age of 65.3 ± 6.4 years. Among them, six were positive for HBs-Ag and six were positive for anti-HCV. Histological examination of these noncancerous liver tissue samples revealed findings compatible with chronic hepatitis in four and cirrhosis in eight.

As a validation cohort, 45 samples of normal liver tissue (C11–C55) exhibiting no remarkable histological findings were obtained from 45 patients without HCCs who were negative for both HBs-Ag and anti-HCV. The patients comprised 34 men and 11 women with a mean age of 62.2 ± 7.0 years. A total of 39 patients underwent partial hepatectomy for liver metastases from primary colon cancer, three patients did so for liver metastasis from gastric cancer and the remaining three patients did so for liver metastasis from each of gastrointestinal stromal tumor of the stomach, pancreatic cancer and colon carcinoid tumor, respectively. A total of 45 samples of noncancerous liver tissue (N13–N57) were obtained from 45 patients who underwent partial hepatectomy for HCCs. The patients comprised 37 men and eight women with a mean age of 62.3 ± 9.7 years. Of them 13 were positive for HBs-Ag, 29 were positive for anti-HCV, and three were negative for both. Histological examination of these noncancerous liver tissue samples revealed findings compatible with chronic hepatitis in 22 and cirrhosis in 23.

For comparison, 34 samples of primary HCC (T1–T34) were also obtained from specimens surgically resected from the patients who had provided the samples N1–N34. In addition, for comparison, 14 samples of liver tissue (V1–V14) were obtained from 14 patients who were positive for HBs-Ag or anti-HCV, but who had never developed HCCs. The patients comprised six men and eight women with a mean age of 65.1 ± 8.2 years. Of them, 12 patients underwent partial hepatectomy for liver metastases of primary colorectal cancer and two patients did so for liver metastases of gastric cancer.

Our study was approved by the Ethics Committee of the National Cancer Center, Tokyo, Japan. All the patients gave informed consent before their inclusion in our study.

DNA extraction and bisulfite DNA modification

High-molecular-weight DNA from fresh-frozen tissue samples was extracted using phenol–chloroform followed by dialysis. Bisulfite conversion was carried out using 1 μg of genomic DNA and the reagents provided in the EpiTect Bisulfite Kit (QIAGEN GmbH, Hilden, Germany), in accordance with the manufacturer's protocol. This process converts unmethylated cytosine residues to uracil, whereas methylated cytosine residues remain unchanged.[21]

Pyrosequencing DNA methylation analysis

DNA methylation level was measured by a highly quantitative method using Pyrosequencing™ technology. Polymerase chain reaction (PCR) and sequencing primers were designed based on the converted sequences using Pyrosequencing Assay Design Software ver.1.0 (QIAGEN GmbH). To overcome PCR bias in DNA methylation analysis, we optimized the annealing temperature as described previously.[22,23] Each of the primer sequences and PCR conditions are given in Supporting Information Table 1. The PCR was carried out with 0.6 units of AmpliTaq Gold (Applied Biosystems, Foster City, CA) using 7.5 ng of bisulfite-treated DNA. The

Table 1. Thirty regions that were able to discriminate noncancerous liver tissues (N) from normal liver tissues (C)

Region	BAC clone ID	Location	Characteristics	Gene	Cutoff value (%)	DNA methylation status[1]	Sensitivity (%)	Specificity (%)
1	RP11–104J13	1p35.2	Noncoding/CpG island	None	25.5	C > N	80.0	66.7
2	RP11–104J13	1p35.2	Noncoding	None	26.0	C > N	90.0	91.7
3	RP11–104J13	1p35.2	First intron/CpG island	SDC3	34.0	C > N	90.0	91.7
4	RP11–104J13	1p35.2	Noncoding	None	88.9	C < N	100	66.7
5	RP11–52I2	1p33	First exon/CpG island	FOXD2	47.5	C > N	90.0	91.7
6	RP11–29M22	1p12	Intron	PHGDH	73.0	C < N	100	50.0
7	RP11–21K1	2q37.1	Noncoding	None	93.0	C > N	80.0	50.0
8	RP11–109B15	5q33.1	Noncoding	None	12.0	C < N	80.0	83.3
9	RP11–112B7	7p13	First intron/CpG island	CAMK2B	45.0	C > N	20.0	91.7
10	RP11–120E20	11p15.4	Intron	ART5	85.0	C > N	50.0	100
11	RP11–120E20	11p15.4	Intron/SINE repeat	NUP98	95.7	C < N	100	75.0
12	RP11–334E6	11q23.3	First exon/CpG island	C1QTNF5	23.7	C < N	100	25.0
13	RP11–334E6	11q23.3	First intron/CpG island	THY1	12.6	C > N	60.0	83.3
14	RP11–17M17	11q25	First intron	OPCML	74.0	C > N	100	91.7
15	RP11–17M17	11q25	First intron	OPCML	79.0	C > N	100	33.3
16	RP11–17M17	11q25	First intron	OPCML	49.7	C > N	70.0	50.0
17	RP11–319E16	12p13.32	Noncoding	None	79.0	C > N	70.0	58.3
18	RP11–319E16	12p13.32	Noncoding/SINE repeat	None	45.0	C > N	100	50.0
19	RP11–1100L3	12q13.13	UTR	ACVRL1	50.0	C < N	90.0	83.3
20	RP11–1100L3	12q13.13	Promoter/CpG island	GRASP	7.0	C > N	80.0	58.3
21	RP11–799O6	12q13.3	UTR	ZBTB39	40.0	C < N	100	91.7
22	RP11–799O6	12q13.3	Noncoding/SINE repeat	None	89.0	C < N	80.0	100
23	RP11–89M4	16p13.3	Noncoding	None	38.0	C < N	70.0	100
24	RP11–89M4	16p13.3	Intron	LOC342346	69.0	C > N	100	33.3
25	RP11–89M4	16p13.3	Exon/CpG island	MGRN1	51.0	C < N	100	100
26	RP11–89M4	16p13.3	Intron	MGRN1	28.0	C < N	100	50.0
27	RP11–89M4	16p13.3	Intron/CpG island	MGRN1	67.0	C < N	100	100
28	RP11–348B12	19p13.3	Intron/CpG island	KDM4B	44.0	C < N	100	100
29	RP11–348B12	19p13.3	Intron/CpG island	KDM4B	94.8	C < N	100	41.7
30	RP11–348B12	19p13.3	Intron/CpG island	KDM4B	94.0	C > N	50.0	91.7

[1]C > N, when the signal ratio was lower than the cutoff value, the tissue sample was considered to be at high risk for carcinogenesis; C < N, when the signal ratio was higher than the cutoff value, the tissue sample was considered to be at high risk for carcinogenesis.

biotinylated PCR product was captured on streptavidin-coated beads (Streptavidin Sepharose™ High Performance; GE Healthcare, Uppsala, Sweden). Quantitative sequencing was run on the PyroMark Q24 (QIAGEN GmbH) using the Pyro Gold Reagents (QIAGEN GmbH) in accordance with the manufacturer's protocol. For each assay, the setup included positive controls (Epitect methylated human control DNA; QIAGEN GmbH) and negative controls (Epitect unmethylated human control DNA; QIAGEN GmbH). The PCR products were separated electrophoretically on 3% agarose gel and stained with ethidium bromide to confirm that specific products of the appropriate size and no nonspecific products were obtained on amplification. Representative pyrograms are shown in Figure 1.

As outlined in Figure 1, the DNA methylation level (%) at each CpG site is given by the following formula:

$$\text{luminescence strength of cytosine} / (\text{luminescence strength of cytosine} + \text{luminescence strength of thymine}) \times 100.$$

Statistics

Significant differences in DNA methylation levels at each of the CpG sites between groups of samples were analyzed using the Mann-Whitney *U* test. Survival curves of patient groups with HCCs were calculated by the Kaplan–Meier method,

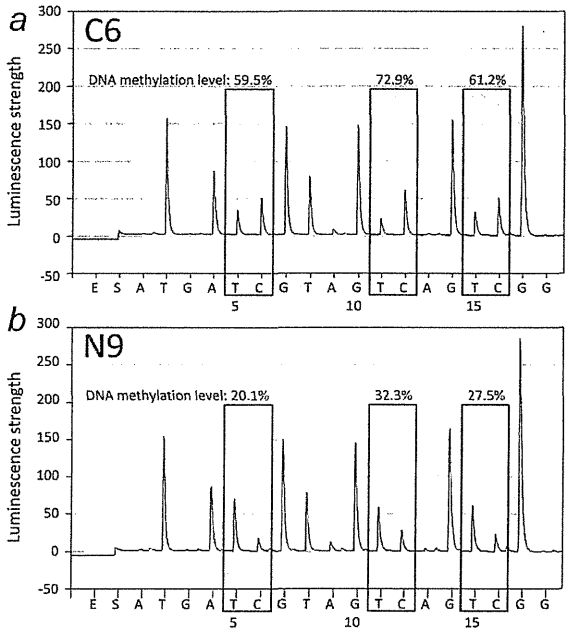

Figure 1. Pyrosequencing DNA methylation analysis. Examples of pyrograms for a sample of normal liver tissue obtained from a patient without HCC (C6) and a sample of noncancerous liver tissue obtained from a patient with HCC (N9) for exon 1 of the *FOXD2* gene (47,677,654, −60, −63 in region 5 in Table 1). Gray columns represent the regions of polymorphic sites after bisulfite modification. *x*-axis indicates dispensation order (time).

and the differences were compared by log-rank test. Differences at $p < 0.05$ were considered significant.

Results

Validation of BAMCA data by pyrosequencing

It has been shown that BAMCA can provide an overview of the DNA methylation tendency of individual large regions among all chromosomes.[13,19] Therefore, using pyrosequencing, we evaluated the DNA methylation levels of all *Xma* I/*Sma* I sites, which yielded less than 2,000 bp PCR products that are effective in BAMCA, on representative BAC clones, which had been identified as indicators for carcinogenetic risk estimation in our previous study.[18] For example, on clone RP11-17M17, there were 10 *Xma* I/*Sma* I sites that were effective in BAMCA (Fig. 2*a*). The average signal ratio by BAMCA of this BAC clone was significantly lower in samples of noncancerous liver tissue obtained from patients with HCCs than in samples of normal liver tissue and was significantly lower in HCCs than in samples of noncancerous liver tissue obtained from patients with HCCs in our previous study.[18] The average DNA methylation levels determined by pyrosequencing of all 10 *Xma* I/*Sma* I sites on this BAC clone in 34 samples of noncancerous liver tissue obtained from patients with HCCs were the same as (*Xma* I/*Sma* I sites i, ii, vii, viii and ix in Fig. 2*a*) or significantly lower than (iii, iv, v, vi and x in Fig. 2*a*) those in 35 samples of normal liver tissue. Moreover, the DNA methylation levels of all *Xma* I/*Sma* I sites in 34 HCCs were significantly lower than those in samples of noncancerous liver tissue obtained from patients with HCCs (i–x in Fig. 2*a*). DNA methylation levels of CpG sites adjacent to the *Xma* I/*Sma* I sites that were quantitatively sequenced using the same sequencing primers tended to be close to the DNA methylation levels of the *Xma* I/*Sma* I sites themselves in each sample, such as iii and iii′ and iv and iv′ in Figure 2*b*. Thus, it was confirmed that BAMCA was able to successfully reveal DNA methylation alterations occurring in a coordinated manner on RP11-17M17. In another BAC clone, RP11-799O6, which was also identified as an indicator for carcinogenetic risk estimation, the average signal ratio obtained by BAMCA was significantly higher in samples of noncancerous liver tissue from patients with HCCs than in samples of normal liver tissue in our previous study.[18] Although the average DNA methylation levels of seven out of 10 *Xma* I/*Sma* I sites, which yielded PCR products of less than 2,000 bp that are effective for BAMCA, by pyrosequencing in samples of noncancerous liver tissue from patients with HCCs were the same as those in samples of normal liver tissue, those of the remaining three *Xma* I/*Sma* I sites in samples of noncancerous liver tissue obtained from patients with HCCs were markedly higher than those in samples of normal liver tissue (data not shown). Thus, pyrosequencing data again validated the BAMCA data for BAC clones identified as indicators for carcinogenetic risk estimation.

Criteria for carcinogenetic risk estimation using liver tissue samples based on pyrosequencing

To identify CpG sites having the largest diagnostic impact, DNA methylation levels of 203 CpG sites were measured by pyrosequencing using primer sets encompassing *Xma* I/*Sma* I sites, which were effective in BAMCA, on the 25 BAC clones on which we based our previous criteria.[18]

On 59 CpG sites, the average DNA methylation levels differed significantly between normal liver tissue and noncancerous liver tissue obtained from patients with HCCs in the learning cohort using Mann-Whitney *U* test ($p < 0.001$). To establish reproducible criteria, 14 CpG sites whose average DNA methylation levels in both normal liver tissue and noncancerous liver tissue obtained from patients with HCCs were less than 10% were omitted from the list of candidate indicators for carcinogenetic risk estimation, taking the characteristics of Pyrosequencing™ technology into consideration.[22] Figure 3*a* shows scattergrams of the DNA methylation levels in samples of normal liver tissue and noncancerous liver tissue obtained from patients with HCCs on representative CpG sites. Using the cutoff values described in each panel, noncancerous liver tissue obtained from patients with

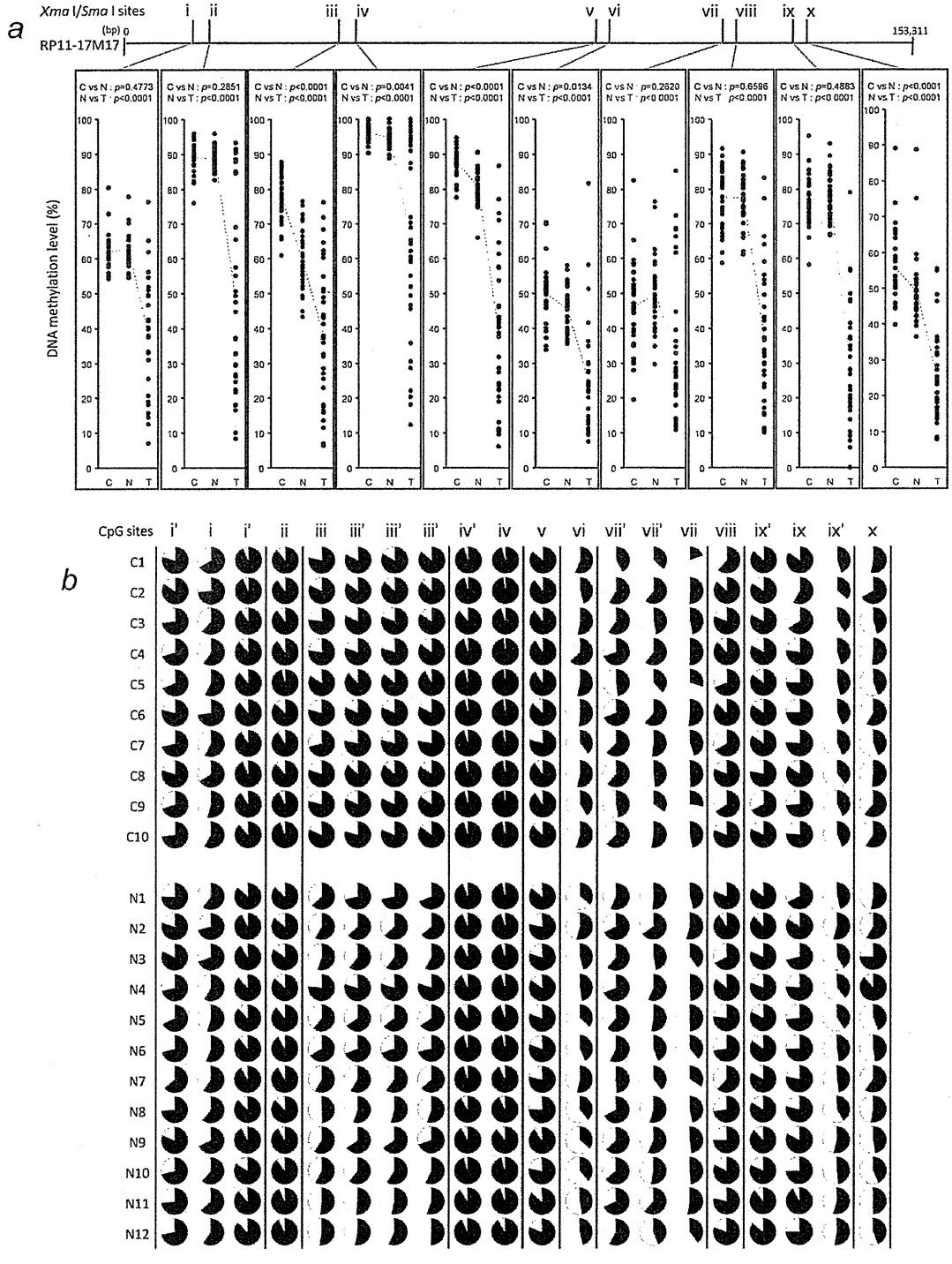

Figure 2. Validation of BAMCA data by pyrosequencing. On RP11-17M17 clone, there were 10 *Xma* I/*Sma* I sites (i–x) that yielded PCR products of less than 2,000 bp that were effective in BAMCA. The average signal ratio obtained by BAMCA for this BAC clone was significantly lower in samples of noncancerous liver tissue obtained from patients with HCCs (N) than in those of normal liver tissue (C) and was significantly lower in HCCs than in N-samples.[18] (*a*) Scattergrams of DNA methylation levels analyzed by pyrosequencing in C-samples (C1–C35), N-samples (N1–N34) and HCCs (T1–T34) on each *Xma* I/*Sma* I site. The average DNA methylation levels obtained by pyrosequencing for all 10 *Xma* I/*Sma* I sites on this BAC clone in 34 N-samples were the same as (on i, ii, vii, viii and ix) or significantly lower than (on iii, iv, v, vi and x) those in 35 C-samples. Moreover, DNA methylation levels in 34 HCCs were significantly lower than those in N-samples (on i–x). (*b*) Pi-charts of DNA methylation levels in C-samples (C1–C10) and N-samples (N1–N12) for each of the CpG sites. CpG sites adjacent to the *Xma* I/*Sma* I site (i, iii, iv, vii and ix), which were quantitatively sequenced using the same sequencing primers, are indicated by i′, iii′, iv′, vii′ and ix′, respectively. White indicates unmethylated cytosine and black indicates methylated cytosine. DNA methylation levels of CpG sites adjacent to the *Xma* I/*Sma* I sites tend to be close to the DNA methylation levels of the *Xma* I/*Sma* I sites themselves, *e.g.*, iii and iii′ and iv and iv′, in each sample.

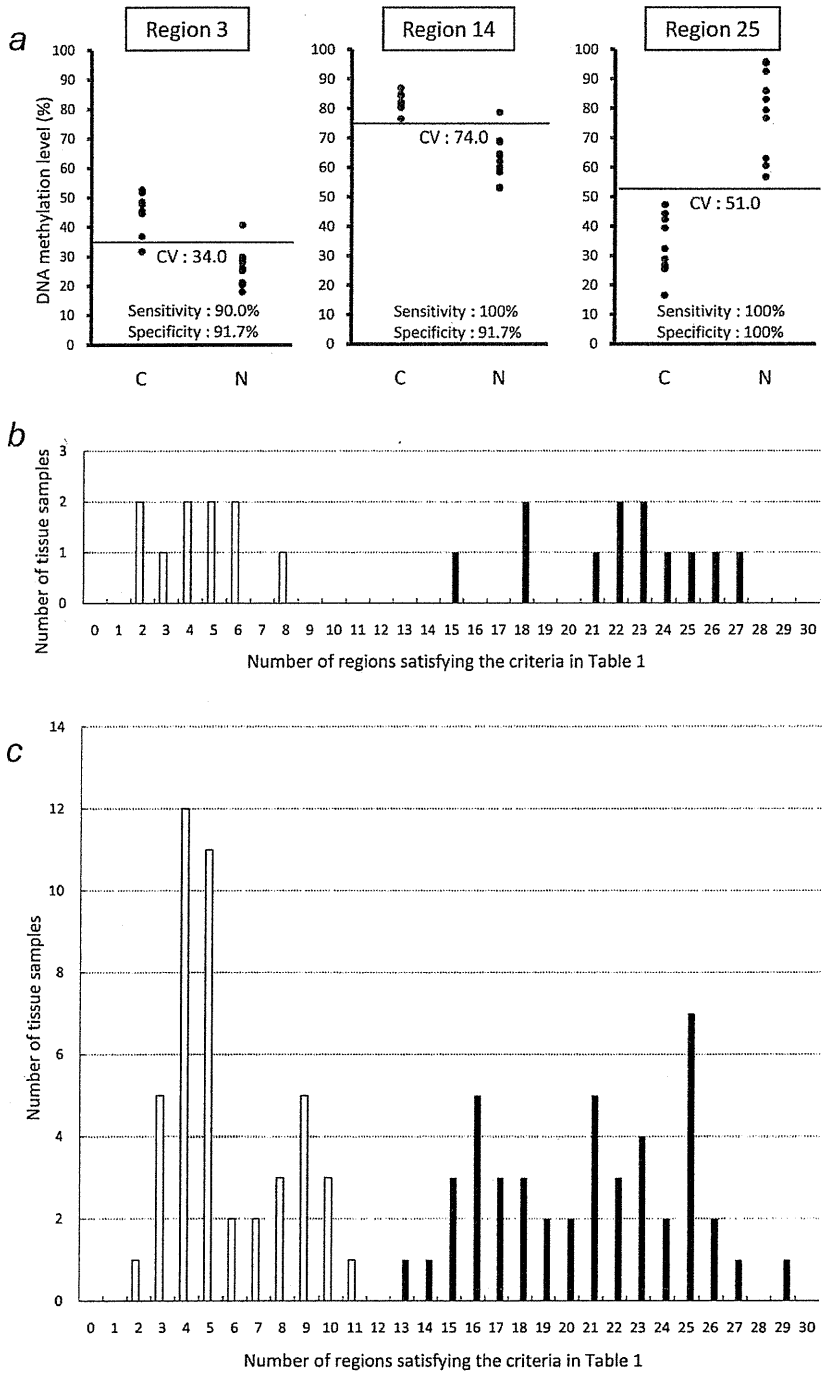

Figure 3. The criteria for carcinogenetic risk estimation based on pyrosequencing. (*a*) Scattergrams of DNA methylation levels in samples of normal liver tissue (C1–C10) and samples of noncancerous liver tissue obtained from patients with HCCs (N1–N12) in the learning cohort for representative regions. Using the cutoff values (CV, %) described in each panel, N-samples in the learning cohort were discriminated from C-samples with sufficient sensitivity and specificity. (*b*) Histogram showing the number of regions satisfying the criteria described in Table 1 in samples C1–C10 (clear columns) and N1–N12 (filled columns). On the basis of this histogram, we judged that when the noncancerous liver tissue satisfied the criteria in Table 1 for 15 or more than 15 regions, it was at high risk of carcinogenesis. (*c*) Validation of the criteria in Table 1 using an additional 90 samples of liver tissue in the validation cohort. All 43 validation samples satisfying the Table 1 criteria for 15 or more regions were N-samples (N13–N36, N38–N41 and N43–N57, filled columns), and 45 of 47 validation samples satisfying the Table 1 criteria for less than 15 regions were C-samples (C11–C55, clear columns). DNA methylation statuses for the 30 regions of N-samples and those of C-samples were completely mutually exclusive in the validation cohort.

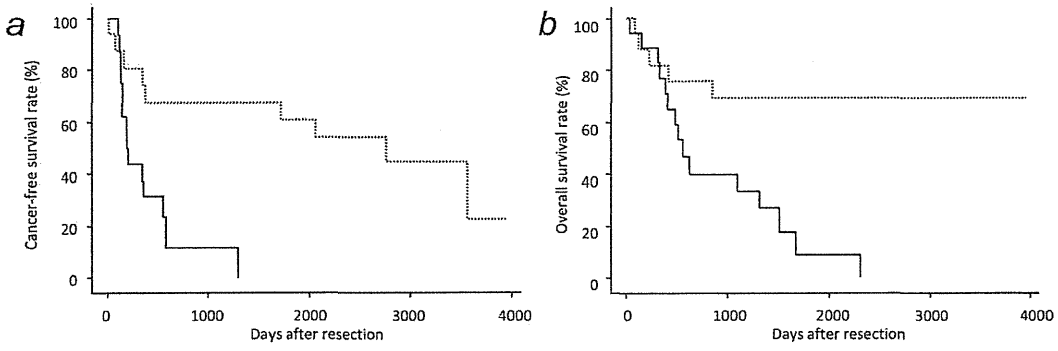

Figure 4. Correlation between DNA methylation status at the precancerous stage and patient outcome. Kaplan–Meier survival curves of patients with HCCs from whom samples N1–N34 were obtained. The cancer-free (*a*; $p = 0.0023$) and overall (*b*; $p = 0.0015$) survival rates of patients with HCCs satisfying the criteria in Table 1 for 23 (the median of the number of regions satisfying the Table 1 criteria) or more than 23 regions in their samples of noncancerous liver tissue ($n = 17$, solid lines) were significantly lower than those of patients with HCCs satisfying the criteria in Table 1 for less than 23 regions ($n = 17$, broken lines).

HCCs in the learning cohort was discriminated from normal liver tissue with sufficient sensitivity and specificity (Fig. 3*a*). On the remaining 45 CpG sites, such discrimination was performed with a sensitivity or specificity of 70% or more than 70%. If several CpG sites were measured using one sequencing primer, one cutoff value was set for the region covered by the sequencing primer using the average DNA methylation levels of the several CpG sites. Then the 30 cutoff values were set for 30 regions including the 45 CpG sites, and their sensitivity and specificity are shown in Table 1. Chromosomal loci and characteristics of the 30 regions (CpG islands or not, exons or introns of specific genes or noncoding regions) are also summarized in Table 1.

A histogram showing the number of regions satisfying the criteria listed in Table 1 for samples C1–C10 and N1–N12 in the learning cohort is shown in Figure 3*b*. On the basis of Figure 3*b*, we finally established that when liver tissue satisfied the criteria in Table 1 for 15 or more regions, it was judged to be at high risk of carcinogenesis. Based on this definition both the sensitivity and specificity for diagnosis of noncancerous liver tissue obtained from patients with HCCs in the learning cohort as being at high risk of carcinogenesis were 100%.

To confirm these criteria, an additional 90 samples of liver tissue were analyzed by pyrosequencing as a validation study (Fig. 3*c*). All of the 43 validation samples satisfying the criteria in Table 1 for 15 or more regions were noncancerous liver tissue obtained from patients with HCCs (N13–N36, N38–N41 and N43–N57), and 45 of the 47 validation samples satisfying the Table 1 criteria for less than 15 regions were normal liver tissue (C11–C55). DNA methylation statuses for the 30 regions of noncancerous liver tissue samples from patients with HCCs and those of normal liver tissue samples were completely mutually exclusive in the validation cohort (Fig. 3*c*), and our criteria enabled diagnosis of noncancerous liver tissue from patients with HCCs in the validation cohort as being at high risk of carcinogenesis with 95.6% sensitivity and 100% specificity.

Clinicopathological significance of DNA methylation status in the 30 regions

To estimate the clinicopathological significance of DNA methylation status in the 30 regions, 34 samples of noncancerous liver tissue from patients with HCCs (N1–N34) in both the learning and validation cohorts for whom follow-up data had been obtained were divided into two groups according to the number of regions satisfying the criteria (≥23 [the median of the number of regions satisfying the Table 1 criteria] regions *vs.* <23 regions). The period covered ranged from 11 to 3,936 days (mean: 1,417 days). The cancer-free and overall survival rates for patients with HCCs satisfying the criteria in Table 1 for 23 or more regions in their noncancerous liver tissue were significantly lower than those of patients with HCCs satisfying the Table 1 criteria for less than 23 regions (Fig. 4, $p = 0.0023$ and $p = 0.0015$, respectively). These data suggested that clinicopathologically valid DNA methylation alterations associated with patient outcome are already present at the precancerous stage.

With respect to all 57 samples of noncancerous liver tissue (N1–N57), the difference in the number of regions satisfying the criteria listed in Table 1 between liver tissue samples showing chronic hepatitis ($n = 26$, 19.6 ± 3.7) and those showing cirrhosis ($n = 31$, 22.0 ± 3.9) was marginal ($p = 0.0206$). For comparison, the DNA methylation levels of 30 regions in 14 additional liver tissue samples (V1–V14) obtained from patients who were infected with HBV or HCV, but who had never developed HCCs, were analyzed by pyrosequencing. The average number of regions satisfying the

Table 1 criteria was significantly lower in V1–V14 (12.0 ± 5.0), than in N1–N57 (20.9 ± 4.0, $p < 0.0001$). These data suggested that our criteria do not simply reflect the presence of hepatitis virus infection, inflammation or fibrosis at the chronic hepatitis and liver cirrhosis stages, but in fact reflect the carcinogenetic risk itself.

Discussion

For appropriate surveillance of patients at the precancerous stage for HCCs, the criteria for carcinogenetic risk estimation should be explored. As considerable numbers of liver tissue samples obtained from patients with HBV or HCV infection indicate a future risk of HCCs, even if HCCs are not yet present, comparison between liver tissue samples obtained from patients with HBV or HCV infection but without HCCs and those obtained from patients with HBV or HCV infection but also showing HCCs, is not an adequate strategy for establishing criteria for carcinogenetic risk estimation. Therefore, in our previous study, we focused on BAC clones whose signal ratios differed significantly between samples of normal liver tissue obtained from patients without HBV or HCV infection and samples of noncancerous liver tissue obtained from patients with HCCs (namely BAC clones on which DNA methylation alterations had occurred at the precancerous stage), and also those on which such DNA methylation alterations had been inherited by HCCs themselves from precancerous conditions. In this way, we successfully established such criteria using BAC array-based methods.[18]

In our study, the reliability of BAMCA was again confirmed: BAMCA was able to provide an overview of DNA methylation tendency in large regions of chromosomes, and especially was able to detect DNA methylation alterations occurring in a coordinated manner in the entire BAC region. However, the exact CpG sites that are of diagnostic impact are unclear, because several *Xma* I/*Sma* I sites that are effective in BAMCA generally exist on each of the BAC clones with an average insert size of 170 kbp.[20] Moreover, as BAMCA requires a large amount of genomic DNA, and the technique is somewhat cumbersome, our previous criteria based on BAMCA may not be suitable for clinical uses such as risk estimation based on liver biopsy specimens. Therefore, we employed Pyrosequencing™ technology, which is an excellent tool for quantitative estimation of DNA methylation levels at specific CpG sites.

Although numerous *Xma* I/*Sma* I sites are located within CpG islands, one or two *Xma* I/*Sma* I sites on each CpG island were analyzed because of difficulties with the design of the PCR and sequencing primers. Then, DNA methylation levels at 203 CpG sites on the 25 BAC clones that comprised our previous criteria based on BAMCA were evaluated quantitatively by pyrosequencing. By combining the 30 regions including 45 specific CpG sites, which were revealed to have a large diagnostic impact, the specificity of the criteria for carcinogenetic risk estimation was successfully improved in comparison with our previous criteria based on BAMCA[18]: the sensitivity and specificity of the criteria after revision by pyrosequencing were both 100% in the learning cohort and were 95.6% and 100% in the validation cohort, respectively.

Only one region (region 20 in Table 1) among 30 regions that had been used for defining the revised criteria for carcinogenetic risk estimation was located within the promoter region of a specific gene (general receptor for phosphoinositides 1-associated scaffold protein), although DNA methylation alterations in promoter regions are known to be one of most consistent epigenetic changes in human cancers.[24] At the risk stage, but not in established cancers, it is feasible that DNA methylation alterations do not expand immediately to the promoter regions of specific genes, such as tumor-related genes. However, 20, 19 and 9 regions that had been used for defining the revised criteria were located within gene bodies, non-CpG islands, and noncoding regions, respectively, which have been overlooked as targets of DNA methylation alterations during multistage human carcinogenesis. Although most of the recently developed detection technologies, such as promoter arrays and CpG island arrays, are sequence-based methods and cannot comprehensively measure the DNA methylation status of gene bodies, non-CpG islands and noncoding regions,[25,26] our findings indicate that meticulous examination of such sequences is also important for establishment of optimal diagnostic indicators.

DNA methylation status in the 30 regions in noncancerous liver tissue at the precancerous stage was significantly correlated with both cancer-free and overall survival rates of patients with HCCs (Fig. 4). Although prognostication before development of HCCs was not a clinically relevant issue, and we never intended to perform such prognostication, we can consider that DNA methylation alterations determining patient outcome had already accumulated at the precancerous stage, based on the data in Figure 4. As DNA methylation status is not randomly altered at the precancerous stage, and DNA methylation profiles in noncancerous liver tissue have been proven to be clinicopathologically valid, it is feasible that such profiles could be optimal indicators for carcinogenetic risk estimation.

The difference in the number of regions satisfying the criteria listed in Table 1 between liver tissue samples showing chronic hepatitis and those showing cirrhosis was marginal, indicating that our criteria were not simply associated with inflammation or fibrosis. In addition, the average number of regions satisfying the Table 1 criteria were significantly lower in liver tissue from patients without HCCs (V1–V14) than in noncancerous liver tissue from patients with HCCs (N1–N34), even though the patients from whom V1–V14 were obtained were infected with HBV or HCV. DNA methylation status in the 30 regions does not depend on hepatitis virus infection but may actually reflect the carcinogenetic risk itself. Therefore, our criteria not only discriminate noncancerous liver tissue from patients with HCCs from normal liver tissues but also may be applicable for classifying liver tissue obtained from patients who are being followed up

because of HBV or HCV infections, chronic hepatitis or cirrhosis into that which may generate HCCs and that which will not.

During surveillance at the precancerous stage, to reveal the baseline liver histology, microscopic examination of liver biopsy specimens is performed in patients with HBV or HCV infection before interferon therapy.[27,28] Therefore, carcinogenetic risk estimation using such liver biopsy specimens will be advantageous for close follow-up of patients who are at high risk of HCC development. We have confirmed that pyrosequencing can be performed using a very small amount of degraded DNA extracted from formalin-fixed and paraffin-embedded liver biopsy specimens (unpublished data). We now intend to prospectively validate the reliability of risk estimation based on the revised criteria using pyrosequencing in liver biopsy specimens obtained before interferon therapy from a large cohort of patients with HBV or HCV infection.

Acknowledgements

Author R.N. received a Research Resident Fellowship from the Foundation for Promotion of Cancer Research in Japan.

References

1. Chang MH, Chen CJ, Lai MS, Hsu HM, Wu TC, Kong MS, Liang DC, Shau WY, Chen DS. Universal hepatitis B vaccination in Taiwan and the incidence of hepatocellular carcinoma in children. Taiwan Childhood Hepatoma Study Group. *N Engl J Med* 1997;336:1855–9.
2. Tanaka Y, Hanada K, Mizokami M, Yeo AE, Shih JW, Gojobori T, Alter HJ. Inaugural article: a comparison of the molecular clock of hepatitis C virus in the United States and Japan predicts that hepatocellular carcinoma incidence in the United States will increase over the next two decades. *Proc Natl Acad Sci USA* 2002; 99:15584–9.
3. Jones PA, Baylin SB. The epigenomics of cancer. *Cell* 2007;128:683–92.
4. Sharma S, Kelly TK, Jones PA. Epigenetics in Cancer. *Carcinogenesis* 2009;31:27–36.
5. Kanai Y, Hirohashi S. Alterations of DNA methylation associated with abnormalities of DNA methyltransferases in human cancers during transition from a precancerous to a malignant state. *Carcinogenesis* 2007;28:2434–42.
6. Kanai Y. Alterations of DNA methylation and clinicopathological diversity of human cancers. *Pathol Int* 2008;58:544–58.
7. Kanai Y, Ushijima S, Tsuda H, Sakamoto M, Sugimura T, Hirohashi S. Aberrant DNA methylation on chromosome 16 is an early event in hepatocarcinogenesis. *Jpn J Cancer Res* 1996;87:1210–7.
8. Kondo Y, Kanai Y, Sakamoto M, Mizokami M, Ueda R, Hirohashi S. Genetic instability and aberrant DNA methylation in chronic hepatitis and cirrhosis—a comprehensive study of loss of heterozygosity and microsatellite instability at 39 loci and DNA hypermethylation on 8 CpG islands in microdissected specimens from patients with hepatocellular carcinoma. *Hepatology* 2000;32:970–9.
9. Kaneto H, Sasaki S, Yamamoto H, Itoh F, Toyota M, Suzuki H, Ozeki I, Iwata N, Ohmura T, Satoh T, Karino Y, Satoh T, et al. Detection of hypermethylation of the p16(INK4A) gene promoter in chronic hepatitis and cirrhosis associated with hepatitis B or C virus. *Gut* 2001; 48:372–7.
10. Saito Y, Kanai Y, Sakamoto M, Saito H, Ishii H, Hirohashi S. Overexpression of a splice variant of DNA methyltransferase 3b, DNMT3b4, associated with DNA hypomethylation on pericentromeric satellite regions during human hepatocarcinogenesis. *Proc Natl Acad Sci USA* 2002;99:10060–5.
11. Saito Y, Kanai Y, Nakagawa T, Sakamoto M, Saito H, Ishii H, Hirohashi S. Increased protein expression of DNA methyltransferase (DNMT) 1 is significantly correlated with the malignant potential and poor prognosis of human hepatocellular carcinomas. *Int J Cancer* 2003;105:527–32.
12. Kanai Y. Genome-wide DNA methylation profiles in precancerous conditions and cancers. *Cancer Sci* 2009;101:36–45.
13. Arai E, Kanai Y. DNA methylation profiles in precancerous tissue and cancers: carcinogenetic risk estimation and prognostication based on DNA methylation status. *Epigenomics* 2010;2: 467–81.
14. Misawa A, Inoue J, Sugino Y, Hosoi H, Sugimoto T, Hosoda F, Ohki M, Imoto I, Inazawa J. Methylation-associated silencing of the nuclear receptor 1I2 gene in advanced-type neuroblastomas, identified by bacterial artificial chromosome array-based methylated CpG island amplification. *Cancer Res* 2005;65:10233–42.
15. Sugino Y, Misawa A, Inoue J, Kitagawa M, Hosoi H, Sugimoto T, Imoto I, Inazawa J. Epigenetic silencing of prostaglandin E receptor 2 (PTGER2) is associated with progression of neuroblastomas. *Oncogene* 2007;26:7401–13.
16. Tanaka K, Imoto I, Inoue J, Kozaki K, Tsuda H, Shimada Y, Aiko S, Yoshizumi Y, Iwai T, Kawano T, Inazawa J. Frequent methylation-associated silencing of a candidate tumor-suppressor, CRABP1, in esophageal squamous-cell carcinoma. *Oncogene* 2007;26:6456–68.
17. Arai E, Ushijima S, Fujimoto H, Hosoda F, Shibata T, Kondo T, Yokoi S, Imoto I, Inazawa J, Hirohashi S, Kanai Y. Genome-wide DNA methylation profiles in both precancerous conditions and clear cell renal cell carcinomas are correlated with malignant potential and patient outcome. *Carcinogenesis* 2009;30:214–21.
18. Arai E, Ushijima S, Gotoh M, Ojima H, Kosuge T, Hosoda F, Shibata T, Kondo Y, Yokoi S, Imoto I, Inazawa J, Hirohashi S, et al. Genome-wide DNA methylation profiles in liver tissue at the precancerous stage and in hepatocellular carcinoma. *Int J Cancer* 2009;125:2854–62.
19. Nishiyama N, Arai E, Chihara Y, Fujimoto H, Hosoda F, Shibata T, Kondo T, Tsukamoto T, Yokoi S, Imoto I, Inazawa J, Hirohashi S, et al. Genome-wide DNA methylation profiles in urothelial carcinomas and urothelia at the precancerous stage. *Cancer Sci* 2010;101: 231–40.
20. Osoegawa K, Mammoser AG, Wu C, Frengen E, Zeng C, Catanese JJ, de Jong PJ. A bacterial artificial chromosome library for sequencing the complete human genome. *Genome Res* 2001;11: 483–96.
21. Clark SJ, Harrison J, Paul CL, Frommer M. High sensitivity mapping of methylated cytosines. *Nucleic Acids Res* 1994;22: 2990–7.
22. Shen L, Guo Y, Chen X, Ahmed S, Issa JP. Optimizing annealing temperature overcomes bias in bisulfite PCR methylation analysis. *Bio Techniques* 2007; 42:48–58.
23. Gao W, Kondo Y, Shen L, Shimizu Y, Sano T, Yamao K, Natsume A, Goto Y, Ito M, Murakami H, Osada H, Zhang J, et al. Variable DNA methylation patterns associated with progression of disease in hepatocellular carcinomas. *Carcinogenesis* 2008;29:1901–10.
24. Baylin SB, Ohm JE. Epigenetic gene silencing in cancer—a mechanism for early oncogenic pathway addiction? *Nat Rev Cancer* 2006;6:107–16.

25. Estecio MR, Issa JP. Tackling the methylome: recent methodological advances in genome-wide methylation profiling. *Genome Med* 2009;1:106.
26. Mohn F, Schubeler D. Genetics and epigenetics: stability and plasticity during cellular differentiation. *Trends Genet* 2009; 25:129–36.
27. Arase Y, Ikeda K, Suzuki F, Suzuki Y, Kobayashi M, Akuta N, Hosaka T, Sezaki H, Yatsuji H, Kawamura Y, Kobayashi M, Kumada H. Comparison of interferon and lamivudine treatment in Japanese patients with HBeAg positive chronic hepatitis B. *J Med Virol* 2007;79: 1286–92.
28. Yoshida H, Tateishi R, Arakawa Y, Sata M, Fujiyama S, Nishiguchi S, Ishibashi H, Yamada G, Yokosuka O, Shiratori Y, Omata M. Benefit of interferon therapy in hepatocellular carcinoma prevention for individual patients with chronic hepatitis C. *Gut* 2004;53: 425–30.

Carcinogenesis vol.32 no.4 pp.462–469, 2011
doi:10.1093/carcin/bgq274
Advance Access publication December 22, 2010

Copy number alterations in urothelial carcinomas: their clinicopathological significance and correlation with DNA methylation alterations

Naotaka Nishiyama[1,2], Eri Arai[1], Ryo Nagashio[1], Hiroyuki Fujimoto[3], Fumie Hosoda[4], Tatsuhiro Shibata[4], Taiji Tsukamoto[2], Sana Yokoi[5], Issei Imoto[5], Johji Inazawa[5] and Yae Kanai[1,*]

[1]Pathology Division, National Cancer Center Research Institute, Tokyo 104-0045, Japan, [2]Division of Urology, Sapporo Medical University, Sapporo 060-8556, Japan, [3]Urology Division, National Cancer Center Hospital, Tokyo 104-0045, Japan, [4]Cancer Genomics Project, National Cancer Center Research Institute, Tokyo 104-0045, Japan and [5]Department of Molecular Cytogenetics, Medical Research Institute and School of Biomedical Science, Tokyo Medical and Dental University, Tokyo 113-8510, Japan

*To whom correspondence should be addressed. Tel: +81 3 3542 2511; Fax: +81 3 3248 2463; Email: ykanai@ncc.go.jp

The aim of this study was to clarify the genetic backgrounds underlying the clinicopathological characteristics of urothelial carcinomas (UCs). Array comparative genomic hybridization analysis using a 244K oligonucleotide array was performed on 49 samples of UC tissue. Losses of 2q33.3–q37.3, 4p15.2–q13.1 and 5q13.3–q35.3 and gains of 7p11.2–q11.23 and 20q13.12–q13.2 were correlated with higher histological grade, and gain of 7p21.2–p21.12 was correlated with deeper invasion. Losses of 6q14.1–q27 and 17p13.3–q11.1 and gains of 19q13.12–q13.2 and 20q13.12–q13.33 were correlated with lymph vessel involvement. Loss of 16p12.2–p12.1 and gain of 3q26.32–q29 were correlated with vascular involvement. Losses of 5q14.1–q23.1, 6q14.1–q27, 8p22–p21.3, 11q13.5–q14.1 and 15q11.2–q22.2 and gains of 7p11.2–q11.22 and 19q13.12–q13.2 were correlated with the development of aggressive non-papillary UCs. Losses of 1p32.2–p31.3, 10q11.23–q21.1 and 15q21.3 were correlated with tumor recurrence. Unsupervised hierarchical clustering analysis based on copy number alterations clustered UCs into three subclasses: copy number alterations associated with genome-wide DNA hypomethylation, regional DNA hypermethylation on C-type CpG islands and genome-wide DNA hypo- and hypermethylation were accumulated in clusters A, B_1 and B_2, respectively. Tumor-related genes that may encode therapeutic targets and/or indicators useful for the diagnosis and prognostication of UCs should be explored in the above regions. Both genetic and epigenetic events appear to accumulate during urothelial carcinogenesis, reflecting the clinicopathological diversity of UCs.

Introduction

Urothelial carcinomas (UCs) are classified as superficial papillary carcinomas or non-papillary carcinomas according to their configuration (1). Papillary carcinomas usually remain non-invasive although patients need to undergo repeated urethrocystoscopic resection for recurrences. In contrast, non-papillary invasive carcinomas usually develop from widely spreading flat carcinomas *in situ* showing a higher histological grade, and their clinical outcome is poor. There is also an alternative pathway by which papillary carcinomas develop higher histological grades during repetitive recurrence and transform into non-papillary invasive carcinomas. Thus, UCs show marked clinicopathological diversity (2). In order to improve the efficiency of diagnosis and therapy, it is necessary to clarify the genetic backgrounds underlying the various clinicopathological characteristics of UCs.

Previous studies employing Southern blotting based on restriction enzyme length polymorphism, polymerase chain reaction (PCR)–loss of heterozygosity (LOH) analysis using microsatellite markers, comparative genomic hybridization (CGH) analysis and fluorescence *in situ* hybridization (FISH) have revealed chromosomal instability in UCs such as losses of 2q, 5q, 9q and 10q and gains of 5p, 7p, 8q, 11q and 20q (3–12). However, such approaches are not effective for defining the break points in detail. Although recently developed array-based technology has been applied to UCs (13–18), the resolution of the arrays employed was insufficient or correlations between copy number alterations and the clinicopathological parameters of UCs were not analyzed in detail. Therefore, the genetic backgrounds underlying urothelial carcinogenesis have not been fully clarified.

In addition, multistage carcinogenesis is known to comprise both genetic and epigenetic events (19–21). We have reported the accumulation of DNA methylation on C-type CpG islands (22) in a cancer-specific, but not age-dependent, manner and demonstrated protein overexpression of DNA methyltransferase 1, a major DNA methyltransferase, even in non-cancerous urothelia with no apparent histological changes obtained from patients with UCs (23,24), as a result of possible exposure to carcinogens in the urine at the precancerous stage. Accumulation of DNA methylation on C-type CpG islands associated with DNA methyltransferase 1 protein overexpression was more frequently evident in aggressive non-papillary UCs (23,24). DNA hypomethylation on pericentromeric satellite regions was significantly correlated with LOH on chromosome 9 in UCs (25). Moreover, we have identified optimal indicators for carcinogenetic risk estimation in histologically normal urothelia, and for prognostication in surgically resected specimens from patients with UCs (26) using the bacterial artificial chromosome array-based methylated CpG island amplification (BAMCA) method (27–29), which is suitable for overviewing the DNA methylation tendency of individual large regions among all chromosomes (30). Although these data indicated that not only genetic but also epigenetic alterations play significant roles in UC development, to our knowledge, the correlations between copy number alterations and DNA methylation profiles in UCs have not been examined in a genome-wide manner.

In the present study of 49 UCs, we analyzed copy number alterations by array CGH analysis using a high-resolution (244K) oligonucleotide array, DNA methylation alterations on a genome-wide scale using BAMCA and DNA methylation status on C-type CpG islands using bisulfite modification. We then examined the clinicopathological significance of copy number alterations and the correlations between alterations of copy number and those of DNA methylation.

Abbreviations: BAC, bacterial artificial chromosome; BAMCA, bacterial artificial chromosome array-based methylated CpG island amplification; CGH, comparative genomic hybridization; COBRA, combined bisulfite restriction enzyme analysis; FISH, fluorescence *in situ* hybridization; LOH, loss of heterozygosity; mRNA, messenger RNA; MINT, methylated in tumor; MSP, methylation-specific polymerase chain reaction; RT, reverse transcription; PCR, polymerase chain reaction; UC, urothelial carcinoma.